


Theory of structural relaxation in glass from the thermodynamics of irreversible processes

Karan Doss* and John C. Mauro[†]

Department of Materials Science and Engineering, The Pennsylvania State University, University Park, Pennsylvania 16802, USA

 (Received 7 March 2021; accepted 12 May 2021; published 9 June 2021)

This work proposes a fundamental thermodynamic description of structural relaxation in glasses by establishing a link between the Prony series solution to volume relaxation derived from the principles of irreversible thermodynamics and asymmetric Lévy stable distribution of relaxation rates. Additionally, it is shown that the bulk viscosity of glass, and not the shear viscosity, is the transport coefficient governing structural relaxation. We also report the distribution of relaxation times and energy barrier heights underpinning stretched exponential relaxation. It is proposed that this framework may be used for qualitative and quantitative descriptions of the relaxation kinetics in glass.

DOI: [10.1103/PhysRevE.103.062606](https://doi.org/10.1103/PhysRevE.103.062606)

I. INTRODUCTION

The nature of glass and the glass transition is widely regarded as one of the most fascinating and important unsolved problems at the cutting edge of condensed matter theory [1–3]. The reverse kinetic process of the glass transition, viz., relaxation in liquids and glasses [4], also remains one of the oldest, most thoroughly studied and yet unsolved problems [3]. These problems are closely related, and modeling relaxation remains a nontrivial task owing to the noncrystalline, nonequilibrium, and nonergodic nature of the glassy state, whose properties are strongly governed by its temperature and pressure histories [5–8]. Relaxation behavior is observed in several processes of technological importance such as volume relaxation (compaction) in liquid crystal displays that limit the achievable pixel density, or the dependence of Rayleigh scattering in optical fibers on the thermal history and relaxation of density fluctuations [9,10]. While stress relaxation plays an important role in limiting ion exchange temperatures during the processing of ion-exchanged glasses, structural relaxation has a large impact on the temporal stability of salient properties of glass articles [11,12]. Both stress and structural relaxation in fact reflect structural changes but a distinction here has been made on the basis of disparate kinetics of the two processes, defined as follows: (a) Stress relaxation refers to the decay of stress within a material subjected to a mechanical impulse in the form of a constant strain, and (b) structural relaxation refers to the response of a material subjected to a thermal impulse measured through observable changes in the material's properties (volume or density, refractive index, etc.) due to structural rearrangements over time [12]. Structural relaxation as measured through changes in the volume (or density) is of particular interest in this work and therefore the process of volume relaxation (densification) will be referred to as structural relaxation in this paper. In glasses

and polymers, the relaxation of thermodynamic properties that have been perturbed out of equilibrium spontaneously relax towards equilibrium following a fat tailed distribution given by the Kohlrausch-Williams-Watts (KWW) stretched exponential function [13–16],

$$\phi(t) = \exp \left[- \left(\frac{t}{\tau_k} \right)^{\beta^*} \right] \quad (1)$$

where τ_k and β^* are the characteristic relaxation time and the dimensionless stretching exponent, respectively.

For stress relaxation experiments, the relaxation time is linked to the shear viscosity through the Maxwell relation [17],

$$\eta_s = G_\infty \langle \tau \rangle = G_\infty \frac{\tau_k}{\beta^*} \Gamma \left(\frac{1}{\beta^*} \right), \quad (2)$$

where η_s is the shear viscosity, G_∞ is the high frequency shear modulus, and $\langle \tau \rangle$ is the average relaxation time. While $\langle \tau \rangle$ is generally referred to as the relaxation time in literature, the relaxation times for stress and structural relaxation for multicomponent glasses can be more than an order of magnitude different from each other at the same temperatures. Doss *et al.* [18] highlighted that this disparity in kinetics could stem from structural relaxation being coupled to *bulk viscosity*, which appears in the Navier-Stokes equation as the coefficient to the divergence of velocity field of the fluid. This was recently supported by an in-depth experimental study on structural relaxation in lead metasilicates [19]. Early estimates for bulk viscosity of glasses were reported by Rekhson [20]. It was reported that the bulk viscosity of single- and two- component systems was less than the shear viscosity while the opposite was found to be true for multicomponent systems. While shear viscosity, its temperature dependence, and connection to relaxation behavior have been thoroughly studied and modeled for decades now, there still exists a dearth of bulk viscosity data for glassy materials. Prior discussions on bulk viscosity span studies related to acoustics [21,22], molecular theories of fluids [23–26], or generalized

*Corresponding author: kud207@psu.edu

†Corresponding author: jcm426@psu.edu

hydrodynamics [27,28]. In fact, the elastic high frequency response of fluids has even engendered elastic theories of the glass transition and relaxation phenomena [29,30]. However, there remains to be no explicit theoretical grounds for bulk viscosity's hypothesized connection to structural relaxation in glass, which motivated the authors to pursue a theoretical basis in this regard. The proposed approach provides a concrete rationale for pursuing further research on bulk viscosity as the salient transport coefficient in structural relaxation of glasses as it perspicuously decouples the kinetics of shear stress relaxation and volume relaxation, relating the latter to bulk viscosity.

The physical significance of the stretching exponent, the second parameter in Eq. (1) has been ascribed to the network topology [16,31], as have many other properties of glass [32–35] with the advent of topological constraint theory [36,37]. Phillips [16], based on Grassberger and Procaccia's interpretation of the diffusion trap problem [38], hypothesized that the stretching exponent is a function of the fractional dimension of the diffusion process involving the diffusion of "excitations" towards randomly distributed static "traps." Quantitatively, this is expressed as

$$\beta^* = \frac{fd}{fd + 2}, \quad (3)$$

where d and f are the dimensionality of the space in which diffusion is taking place and the fraction of activated relaxation pathways, respectively. Phillips [16], based on a thorough literature survey of relaxation data, also proposed "magic" values for β^* at low temperatures which were reported to be $3/5$ for stress relaxation ($d = 3$ and $f = 1$) and $3/7$ for structural relaxation ($d = 3$ and $f = 0.5$). This result has been experimentally confirmed [31,39], and points to fundamentally different mechanisms governing the two relaxation phenomena as they appear to correspond to different effective dimensionalities.

Aside from the aforementioned diffusion trap model, other salient efforts in the pursuit of analytically deriving the stretched exponential relaxation function include the Förster direct-transfer model [40], a parallel channel relaxation model that arose from studies of excitation transfers from donor to static defects in condensed media, the hierarchically constrained dynamics model proposed Palmer *et al.* [41], a serial relaxation model that supposes that relaxation occurs in stages wherein the faster degrees of freedom must relax first (thereby imposing a constraint on the slower degrees of freedom), and the defect-diffusion model proposed by Glarum [42] which suggests that migrating defects trigger the relaxation of frozen dipoles in amorphous materials. These are by no measure the only models and a quick literature survey is sure to yield plenty of theoretical models that naturally give rise to the stretched exponential. Unlike the more abstract diffusion trap model, the aforementioned models are rooted in a physical mechanism that describes the dynamics of a system relaxing in response to a certain excitation. These models also introduce a more palatable interpretation of the stretching exponent (β^*) relative to the more abstraction notion of a "fraction of relaxation pathways" discussed in the Phillips diffusion trap model. Klafter and Shlesinger [43] very elegantly summarized that the unifying feature within these different physical

models is the generation of a scale-invariant distribution of relaxation times, whose exponent is inevitably related to β^* . Another important conclusion, within the context of this work, from the common underlying mathematical framework underpinning these models is the equivalence of the resulting relaxation function for parallel channel and serial relaxation models.

There is, however, no connection between scale-invariant distributions of relaxation times and a thermodynamic description of structural relaxation with the partial exception of the random first order transition theory [44–46]. The statistical mechanical theory describes supercooled liquids as consisting of domains of glassy clusters whose fluctuations are entropically driven. It appears to predict the existence of spatial scale invariance of cooperatively rearranging regions [47] at relatively elevated temperatures (relative to the glass transition temperature T_g) wherein anomalous particles of clusters relax as stretched exponentials but yield perplexing exponential tails [48] for the distribution of relaxation times. However, a macroscopic thermodynamic description of this phenomenon that is capable of making such a connection is missing, and the authors believe that there is scope for establishing this through the Prony series approximation to the stretched exponential function.

The Prony series often serves as an approximation to the stretched exponential in applications such as modeling viscoelasticity [49] and the evolution of the nonequilibrium state of a glass subjected to unique thermal histories [50,51]. The latter application involves estimating the fictive temperature (T_f), a fictitious temperature at which the glassy state could be mapped to an equivalent liquid. Broadly speaking, there are three interpretations for the fictive temperature, viz., microscopic, macroscopic, and kinetic (refer to Ref. [52] for definitions). Many attempts have been made to rigorously quantify the fictive temperature through experimentally measurable properties [53–55] in an attempt to standardize the description of a nonequilibrium state with a single thermodynamic state variable. However, it was famously shown by Ritland [56] that a single fictive temperature was in essence insufficient to accurately capture the nonequilibrium state of a glass as one encountered crossover effects (such as those shown in Fig. 1) when two glasses with identical fictive temperatures are prepared through dissimilar thermal histories. To this end, the kinetic interpretation of fictive temperature, which purports that there exist multiple fictive temperatures (partial fictive temperature components) that represent different relaxation modes within the glass, found great success within the glass community with regard to relaxation modeling [49–51]. The Prony series in this case arises from modeling the kinetic fictive temperature as a linear superposition of partial fictive temperatures that evolve as a set of coupled first order differential equations [50,51].

Prony's method, like the Fourier transform, is used to decompose a uniformly sampled time domain signal [$M(t)$] into a sum of damped complex exponentials. The Prony series is a homogenous solution to a linear differential equation, and Prony's method allows for the direct estimation of frequency, damping, strength, and relative phase of modal components in a signal [57]. The Prony series (for zero phase and positive

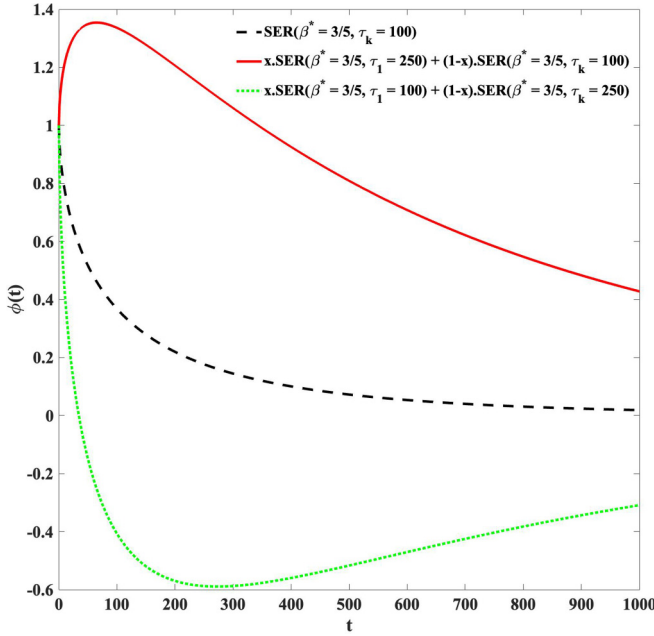


FIG. 1. Solutions to Eq. (36) may result in nonmonotonic or crossover type relaxation responses (solid red and dotted green lines) in contrast with a monotonic stretched exponential decay (dashed black line). Here, $\text{SER}(\tau, \beta^*) = \exp[-(t/\tau)^{\beta^*}]$ where SER stands for stretched exponential relaxation and $x = v(t=0)/[v(t=0) - v^0]$.

system eigenvalues) is expressed as

$$M(t) = \sum_{i=1}^m w_i e^{-K_i(t/\tau_k)}, \quad (4)$$

where w_i and K_i ($i = 1, 2, \dots, m$) are the parameters of the Prony series that may be optimized to fit such a time domain signal. For a stretched exponential function ($M(t) \sim \exp[-(t/\tau_k)^{\beta^*}]$), an additional constraint of $\sum_i w_i = 1$ is imposed where w_i are the amplitudes of the modal components and K_i are the eigenvalues of the system which have been normalized by a characteristic frequency $\lambda^* = 1/\tau_k$. The state-of-the-art technique to model relaxation behavior and the subsequent estimation of the isostructural viscosity considers a weighted average of fictive temperature components ($T_{f,i}$) to estimate the fictive temperature [32]

$$T_f = \sum_{i=1}^N w_i T_{f,i}, \quad (5)$$

where w_i are the weights obtained from Eq. (4). The fictive temperature components evolve as a set of coupled first order differential equations,

$$\frac{dT_{f,i}}{dt} = -\frac{T_{f,i}(t) - T(t)}{\tau_i [T_{f,i}(t), T(t)]}, \quad (6)$$

where the relaxation time of each component is $\tau_i = \tau_k/K_i$, wherein K_i is obtained from Eq. (4). While there have been some notable attempts to incorporate the concept of fictive temperature into an irreversible thermodynamics framework by Gupta and Moynihan [58,59], it still remains to be a purely mathematically convenient way to model relaxation behavior

wherein the Prony series is used to fit the stretched exponential function. To the best of the authors knowledge, there is still no physical interpretation for the fitting parameters w_i and K_i that stems from a rigorous thermodynamic standpoint. However, recent work by Mauro and Mauro [50] offers quantitative insights that will form the basis of some of the results presented here.

This paper addresses three important aspects of structural relaxation, viz., (i) the role of bulk viscosity, as opposed to shear viscosity governing the volume relaxation process which would explain the departure of structural relaxation times from relaxation times obtained using the Maxwell relation through the isostructural viscosity, (ii) presenting a thermodynamic basis for the kinetic interpretation of fictive temperature, and (iii) presenting distributions of relaxation times and energy barrier heights underpinning stretched exponential relaxation and discussing their implications for microscopic theories for structural relaxation. The intention with this work is to (i) build a firm theoretical foundation upon which future experimental and computational relaxation studies may be designed, (ii) offer insights into a potential microscopic theory of relaxation that is consistent with the macroscopic thermodynamics presented here, and (iii) implement the results presented here into physics based open-source relaxation software such as RELAXPY [51] that can model isostructural viscosity [55,60] of glasses subjected to specific temperature paths.

The organization of the paper is as follows. Section II introduces the general entropy balance equation derived from conservation equations. Although these are well documented results, the authors include this background knowledge because results from this section will be used in subsequent sections. In Sec. III, symmetry principles are leveraged to decouple entropy generation sources of dissimilar tensorial character. This section cements the kinetic decoupling of shear and bulk viscous flows. The subsequent Sec. IV discusses the rate equations for structural relaxation and highlights the relationship between bulk viscosity and structural relaxation. Section V discusses the relationship between the Prony series solution for the proposed rate equations and offers physical insights into the fitting parameters of the Prony series. Section VI discusses Lévy stable distributions that naturally arise from the Prony series for stretched exponential relaxation and presents distributions of relaxation times and energy barrier heights. The paper ends with a brief discussion in Sec. VII followed by concluding remarks in Sec. VIII.

II. CONSERVATION LAWS AND ENTROPY BALANCE

An irreversible thermodynamic description of a system (whose properties are continuous functions of space and time) is founded on a combination of the first and second laws of thermodynamics, conservation of mass, and conservation of momentum. The conservation laws have been discussed systematically below and important results that pertain to the discussion at hand have been presented here. The reader is advised to refer to Ref. [61] for a more detailed discussion and derivation of the conservation laws. Consider an n -component system with “ r ” possible chemical reactions. The rate of change of mass component “ k ” within a volume V is given

by

$$\int_V \frac{\partial \rho_k}{\partial t} dV = - \int_{\Omega} \rho_k \mathbf{v}_k \cdot d\boldsymbol{\Omega} + \sum_{j=1}^r \int_V v_{kj} J_j dV, \quad (7)$$

where ρ_k is the density of component k (mass per unit volume), $d\boldsymbol{\Omega}$ is the vector with magnitude $d\Omega$ normal to the surface counted positive pointing outward (inside to outside), \mathbf{v}_k is the velocity of component k , and $v_{kj} J_j$ is the production (mass) of component k in the j th reaction. The first term accounts for the net flow of k into volume V and the second term accounts for the total production of k inside the volume element V . The v_{kj} term normalized by the molar mass of k is proportional to the stoichiometric coefficient of k in reaction j such that it is positive if k is a product (right hand side of a chemical equation) and negative if k is a reactant (left hand side of a chemical equation). The mass balance condition necessitates that $\sum_k v_{kj} = 0$. The rate of reaction J_j has units of mass per unit volume per unit time. Applying Gauss' law to Eq. (7), one obtains the following expression:

$$\frac{\partial \rho_k}{\partial t} = -\nabla \cdot (\rho_k \mathbf{v}_k) + \sum_{j=1}^r v_{kj} J_j \quad (k = 1, 2, \dots, n). \quad (8)$$

Summing Eq. (8) over k one obtains

$$\frac{\partial \rho}{\partial t} + \nabla \cdot (\rho \mathbf{v}) = 0, \quad (9)$$

where the density $\rho = \sum_k \rho_k$ and the barycentric velocity $\mathbf{v} = \sum_k \rho_k \mathbf{v}_k / \rho$. Then one may define the mass fraction of k as $c_k = \rho_k / \rho$ with associated diffusion flow of k , $\mathbf{J}_k = \rho_k (\mathbf{v} - \mathbf{v}_k)$ with respect to the barycentric motion in order to obtain the following equation for the generation of k within a volume V :

$$\rho \frac{dc_k}{dt} = -\nabla \cdot \mathbf{J}_k + \sum_{j=1}^r v_{kj} J_j. \quad (10)$$

It follows from the definitions of \mathbf{v} and \mathbf{J}_k that

$$\sum_k \mathbf{J}_k = 0, \quad (11)$$

which would imply that only $n - 1$ of the n diffusion flows are independent. Additionally, it may be shown that Eq. (9) is equivalent to

$$\frac{1}{v} \frac{dv}{dt} = \nabla \cdot \mathbf{v}, \quad (12)$$

where $v = \rho^{-1}$ is the specific volume.

Conservation of energy implies that the total energy content within an arbitrary volume V in the system will change if there is an influx (or outflux) of energy through its boundary Ω ,

$$\frac{d}{dt} \int_V \rho e dV = \int_V \frac{\partial \rho e}{\partial t} dV = - \int_{\Omega} \mathbf{J}_e \cdot d\boldsymbol{\Omega}, \quad (13)$$

where \mathbf{J}_e is the total energy flux per unit surface per unit time and e is the total specific energy (energy per unit mass) which consists of contributions from the specific kinetic energy ($v^2/2$), specific potential energy (ψ), and specific internal

energy (u),

$$e = \frac{1}{2} \mathbf{v}^2 + \psi + u. \quad (14)$$

From these equations, one may derive an equation for the first law of thermodynamics of the form

$$\frac{du}{dt} = \frac{dq}{dt} - p \frac{dv}{dt} - v \tilde{\boldsymbol{\Pi}} : \nabla \mathbf{v} + v \sum_k \mathbf{J}_k \cdot \mathbf{F}_k, \quad (15)$$

where dq is the heat added per unit mass and

$$\rho \frac{dq}{dt} = -\nabla \cdot \mathbf{J}_q, \quad (16)$$

where \mathbf{J}_q is the heat flow. $\mathbf{F}_k = -\nabla \psi_k$ is the force per unit mass exerted on chemical component k and contains contributions from external forces and possible long-range interactions in the system. No nonconservative forces have been taken into account, i.e., \mathbf{F}_k is a conservative force derived from a potential ψ_k such that $\partial \psi_k / \partial t = 0$. The terms p and $\tilde{\boldsymbol{\Pi}}$ come from the decomposition of the total pressure tensor $\mathbf{P} = p \mathbf{I}_3 + \tilde{\boldsymbol{\Pi}}$, where p is the scalar hydrostatic part and $\tilde{\boldsymbol{\Pi}}$ is a viscous stress tensor. \mathbf{P} is thought to result from short range interactions between particles of the system. The tensor notation “:” corresponds to the Frobenius inner product of two tensors.

The change in entropy (dS) may be written as a sum of entropy supplied to a system by its surroundings ($d_e S$) and the entropy produced inside the system ($d_i S$),

$$dS = d_e S + d_i S, \quad (17)$$

wherein the second law of thermodynamics necessitates that $d_i S > 0$ for irreversible processes and $d_e S = \delta Q / T$ for a closed system. For an arbitrary system volume V , the following relation must be valid:

$$\int_V \left(\frac{\partial \rho s}{\partial t} + \nabla \cdot \mathbf{J}_{s,\text{tot}} - \sigma \right) dV = 0, \quad (18)$$

where s is the entropy per unit mass, $\mathbf{J}_{s,\text{tot}}$ is the total entropy flow per unit area per unit time, and $\sigma \geq 0$ is the entropy source strength or entropy production per unit volume per unit time. The first term in Eq. (18) arises from the time rate of change of the total entropy, the second term arises from $d_e S / dt$, and the third term from $d_i S / dt$. Equation (18) can now be rewritten as

$$\rho \frac{ds}{dt} = -\nabla \cdot \mathbf{J}_s + \sigma, \quad (19)$$

where the entropy flux, $\mathbf{J}_s = \mathbf{J}_{s,\text{tot}} - \rho s \mathbf{v}$. Equation (19) is the desired form of the entropy balance equation.

III. CURIE SYMMETRY PRINCIPLE AND ENTROPY GENERATION EQUATION FOR ISOTROPIC MEDIA

To relate the conservation equations to the rate of change of entropy per unit mass, one considers $s = s(u, v, c_k)$ so as to write the total differential of s using the Gibbs relation,

$$T ds = du + p dv - \sum_{k=1}^n \mu_k dc_k, \quad (20)$$

where p is the equilibrium pressure and μ_k is the chemical potential for component k which is a partial specific Gibbs

function. Assuming local equilibrium wherein Eq. (20) is valid for a small mass element followed along its center of gravity motion yields

$$T \frac{ds}{dt} = \frac{du}{dt} + p \frac{dv}{dt} - \sum_{k=1}^n \mu_k \frac{dc_k}{dt}. \quad (21)$$

Equation (21) is thought to be valid for systems near equilibrium and microscopic considerations for certain systems allow for deriving the limits of validity of this equation. Plugging in Eqs. (10), (15), and (16) into Eq. (21), one obtains the explicit form of entropy balance equation,

$$\rho \frac{ds}{dt} = -\nabla \cdot \left(\frac{\mathbf{J}_q - \sum_k \mu_k \mathbf{J}_k}{T} \right) - \frac{1}{T^2} \mathbf{J}_q \cdot \nabla T - \frac{1}{T} \sum_k \mathbf{J}_k \cdot \left[T \nabla \left(\frac{\mu_k}{T} \right) - \mathbf{F}_k \right] - \frac{1}{T} \tilde{\Pi} : \nabla \mathbf{v} - \frac{1}{T} \sum_{j=1}^r J_j A_j, \quad (22)$$

where the chemical affinity $A_j = \sum_{k=1}^n v_{kj} \mu_k$.

Comparing Eq. (22) with Eq. (19) and using the relation

$$\mathbf{J}'_q = \mathbf{J}_q - \sum_{k=1}^n h_k \mathbf{J}_k, \quad (23)$$

where h_k is the partial specific enthalpy of component k , the expression for the entropy flux is

$$\mathbf{J}_s = \frac{1}{T} \left(\mathbf{J}_q - \sum_k \mu_k \mathbf{J}_k \right), \quad (24)$$

and for the entropy production is

$$\begin{aligned} \sigma &= -\frac{1}{T^2} \mathbf{J}'_q \cdot \nabla T \\ &\quad - \frac{1}{T} \sum_k \mathbf{J}_k \cdot \{T(\nabla \mu_k)_T - \mathbf{F}_k\} \\ &\quad - \frac{1}{T} \tilde{\Pi} : \nabla \mathbf{v} - \frac{1}{T} \sum_{j=1}^r J_j A_j, \end{aligned} \quad (25)$$

where h_k is the partial specific enthalpy of component k . However, in order to observe the influence of symmetry properties on the phenomenological equations, the entropy production equation must be modified appropriately. The symmetric viscous pressure tensor ($\tilde{\Pi}$) is further decomposed to

$$\tilde{\Pi} = \Pi \mathbf{I}_3 + \dot{\tilde{\Pi}}, \quad (26)$$

where $\Pi = (1/3)\text{Tr}(\tilde{\Pi})$, $\text{Tr}(\dot{\tilde{\Pi}}) = 0$, and the gradient of velocity is expressed as

$$\nabla \mathbf{v} = \frac{1}{3} \nabla \cdot \mathbf{v} \mathbf{I}_3 + (\dot{\nabla} \mathbf{v})^s + (\dot{\nabla} \mathbf{v})^a, \quad (27)$$

where $\dot{\nabla} \mathbf{v}$ is a matrix containing only off-diagonal elements of the gradient of the barycentric velocity. A superscript “s” indicates the symmetric part and “a” indicates the antisymmetric part of the matrix. Then the following expression is obtained:

$$\tilde{\Pi} : \nabla \mathbf{v} = \dot{\tilde{\Pi}} : (\dot{\nabla} \mathbf{v})^s + \Pi \nabla \cdot \mathbf{v}. \quad (28)$$

Substituting Eq. (28) into Eq. (25),

$$\begin{aligned} \sigma &= -\frac{1}{T^2} \mathbf{J}'_q \cdot \nabla T - \frac{1}{T} \sum_k \mathbf{J}_k \cdot \{T(\nabla \mu_k)_T - \mathbf{F}_k\} \\ &\quad - \frac{1}{T} \dot{\tilde{\Pi}} : (\dot{\nabla} \mathbf{v})^s - \frac{\Pi}{T} \nabla \cdot \mathbf{v} - \frac{1}{T} \sum_{j=1}^r J_j A_j. \end{aligned} \quad (29)$$

Therefore, the total contribution of viscous phenomena to the entropy production has been split into shear and dilatational contributions. Additionally, the entropy production equation is expressed as the sum of products of a flux and a conjugate thermodynamic driving force. The entropy production expression also consists of fluxes and forces of different tensorial character, which have specific implications on the coupling between various fluxes when the symmetry of the system is taken into consideration. In fact, according to the Curie symmetry principle, fluxes of different tensorial character do not couple to forces of dissimilar tensorial character. This is because not all tensors behave the same under operations of reflections and rotations, which has the implication that the kinetic coefficients coupling the dissimilar flux-force pairs reduce to zero when their coordinates are transformed through reflections and rotations. Therefore, the entropy production is split up into three distinct sources of generation: (a) the scalar processes of bulk viscous flow, chemical reactions, and their cross effects; (b) viscous flow under shear deformation; and (c) vectoral phenomena of heat conduction, diffusion, and their cross effects. Since the process of volume relaxation does not consist of macroscopic concentration gradients, applied shear stresses, and thermal gradients, the only source of entropy generation is then related to the processes of bulk viscous flow, chemical reactions, and their cross effects:

$$\sigma_0 = -\frac{\Pi}{T} \nabla \cdot \mathbf{v} - \frac{1}{T} \sum_{j=1}^r J_j A_j. \quad (30)$$

Plugging in Eq. (12) into Eq. (30) gives the required result,

$$\sigma_0 = -\frac{\Pi}{T} \frac{1}{v} \frac{dv}{dt} - \frac{1}{T} \sum_{j=1}^r J_j A_j. \quad (31)$$

IV. PHENOMENOLOGICAL EQUATIONS FOR STRUCTURAL RELAXATION AND BULK VISCOSITY

Knowing that symmetry considerations decouple all other cross effects from the process of bulk viscous flow and chemical reactions, one may proceed to select thermodynamic variables in the near equilibrium description to achieve the target entropy production equation (31) as well as associated phenomenological rate equations describing the relaxation of volume and mass fractions of various chemical species in the system. In essence, the proposition is to model structural relaxation as a process wherein salient structural units undergo transformations that result in volume changes (i.e., they are kinetically coupled to the volume and each other). Variables α_i are selected such that they represent departure of specific extensive properties from their equilibrium supercooled liquid

values (marked with superscript “0”),

$$\begin{aligned}\alpha_1 &= v - v^0, \\ \alpha_2 &= c_1 - c_1^0, \\ &\vdots \\ \alpha_{n+1} &= c_n - c_n^0,\end{aligned}\quad (32)$$

where the mass fractions c_k are specifically the mass fractions of salient structural and superstructural units that are involved in the relaxation process. The explicit definition of these structural units is intentionally generic as the precise meaning depends on the type of glass chemistry one is interested in characterizing and there may be arbitrarily many salient structures. This has been discussed in more detail at the end of this section in the context of atomic level stress. The Gibbs relation in Eq. (20) is used to derive driving forces that correspond to fluxes in α_i type variables,

$$\begin{aligned}X_1 &= \frac{\partial \Delta s}{\partial \alpha_1} = \frac{P^i}{T} - \frac{P^0}{T} = -\frac{\Pi}{T}, \\ X_2 &= \frac{\partial \Delta s}{\partial \alpha_2} = -\left(\frac{\mu_1}{T} - \frac{\mu_1^0}{T}\right) = -\frac{\Delta \mu_1}{T}, \\ &\vdots \\ X_{n+1} &= \frac{\partial \Delta s}{\partial \alpha_{n+1}} = -\left(\frac{\mu_n}{T} - \frac{\mu_n^0}{T}\right) = -\frac{\Delta \mu_n}{T},\end{aligned}\quad (33)$$

where P^i is the initial pressure and Π , the mean normal stress, is taken to be positive when compressive. The corresponding entropy generation per unit volume given by the sum of products of fluxes and affinities per unit volume is

$$\rho \frac{d\Delta s}{dt} = -\frac{\Pi}{T} \frac{1}{v} \frac{dv}{dt} - \sum_{k=1}^n \rho \frac{dc_k}{dt} \frac{\Delta \mu_k}{T}.\quad (34)$$

Inserting Eq. (10) into Eq. (34) and comparing with Eq. (19), one obtains the same entropy source term as in Eq. (31), noting that $-\nabla \cdot \mathbf{J}_s = \sum_{k=1}^n \mu_k T^{-1} \nabla \cdot \mathbf{J}_k$ in the absence of temperature gradients based on Eq. (24). Further, the fluxes ($d\alpha_i/dt$) may be expressed as the sum of products of kinetic coefficients [$L_{im}(i, m = 1, 2, \dots, n+1)$] and their corresponding affinities [$X_m(m = 1, 2, \dots, n+1)$],

$$\frac{d\alpha_i}{dt} = \sum_{m=1}^{n+1} L_{im} X_m.\quad (35)$$

However, an alternative expression exists where the fluxes may be expressed as the sum of products of phenomenological coefficients [$M_{im}(i, m = 1, 2, \dots, n+1)$] and their corresponding α_i 's,

$$\frac{d\alpha_i}{dt} = -\sum_{m=1}^{n+1} M_{im} \alpha_m,\quad (36)$$

where the elements [$L_{im}(i, m = 1, 2, \dots, n+1)$] of the kinetic coefficient matrix (\mathbf{L}) are related to the elements [$M_{im}(i, m = 1, 2, \dots, n+1)$] of the phenomenological coefficient matrix (\mathbf{M}) as

$$L_{im} = \sum_{m=1}^{n+1} M_{im} \tilde{g}_{mi}.\quad (37)$$

Here, $\tilde{g}_{mi}(m, i = 1, 2, \dots, n+1)$ are the elements of \mathbf{G}^{-1} , the right inverse of \mathbf{G} , where \mathbf{G} is the matrix of second derivatives of the entropy difference (ΔS) between the nonequilibrium and equilibrium states with respect to the α variables. According to Onsager's reciprocal relations, \mathbf{L} is symmetric in addition to being positive definite. Similarly, \mathbf{G} and its inverse are symmetric and positive definite matrices. Therefore, one may infer that the phenomenological coefficient matrix $\mathbf{M} = \mathbf{L} \times \mathbf{G}$ is positive definite. Therefore, all of the eigenvalues (λ_m) of \mathbf{M} are positive and correspond to the inverse of a relaxation time ($\tau_m = \lambda_m^{-1}$).

The relationship between structural relaxation and bulk viscosity will be examined next. Rearranging Eq. (35) for $i = 1$ and multiplying both sides of the equation by ρ ,

$$\Pi = -\left(\frac{T}{\rho L_{11}}\right) \frac{1}{v} \frac{dv}{dt} - \sum_{k=1}^n \left(\frac{L_{1(k+1)}}{L_{11}}\right) \Delta \mu_k,\quad (38)$$

which is merely another phenomenological realization of the scalar processes of bulk viscous flow, chemical reactions, and their cross effects based on Eq. (34). Additionally, it is known that the volumetric strain rate $\dot{\epsilon}_v = v^{-1}(dv/dt)$, and the bulk viscosity $\eta_v = T(\rho L_{11})^{-1}$ wherein the dependence on specific volume is negligible for small strains which is certainly the case for structural relaxation in glasses. In fact, Ref. [61] [Eq. (17) in Sec. V] presents Eq. (38) in a similar manner but with no dependence of η_v on v . Incorporating these definitions and rearranging the terms in Eq. (38) gives

$$\Pi + \sum_{k=1}^n \left(\frac{L_{1(k+1)}}{L_{11}}\right) \Delta \mu_k = -\eta_v \dot{\epsilon}_v.\quad (39)$$

One can infer from Eq. (39) that there is an internal stress P_{int} generated by chemical potential differences of salient structural and superstructural units between the nonequilibrium glassy state and the supercooled liquid state. Therefore, in the absence of an applied mean hydrostatic stress (i.e., $\Pi = 0$) the relaxation will solely be driven by the structural transformations within the glass. This is exactly the scenario encountered in isothermal-isobaric laboratory volume relaxation studies, and therefore the nonequilibrium bulk viscosity for a glass whose volume exhibits stretched exponential relaxation in such an experiment can be estimated using the bulk analog of the Maxwell relation,

$$\eta_{V,\text{neq}} = \frac{\tau_k}{\beta^*} \Gamma\left(\frac{1}{\beta^*}\right) (K_{\infty,\text{neq}} - K_{0,\text{neq}}) = -\frac{(\Pi + P_{\text{int}})}{\dot{\epsilon}_v},\quad (40)$$

where K_{∞} is the instantaneous bulk modulus, K_0 is the inverse of the compressibility of the system (or the static bulk modulus), $\Pi = 0$, and the “neq” subscript refers to the nonequilibrium property of the glass. Other scenarios where this theoretical framework may be corroborated by experimental results are indenter experiments [62] or relaxation studies involving pressure quenched glasses [6–8] wherein hydrostatic stress fields are imposed on the system. The mean normal stress will be nonzero and must be accounted for when considering bulk viscosity calculations in these scenarios.

The bulk viscosity is assumed to be constant in Eq. (39) but it is known that the viscosity relaxes during the relaxation

process. Ideally one must incorporate the time dependence of the driving forces and (or) kinetic coefficients in Eqs. (35) or (36) and solve the equations accordingly. However, the determination of the nonequilibrium bulk viscosity can be resolved in the current framework as follows. If the system is allowed to relax starting at time $t = 0$ and is then instantaneously quenched, $t = t_1$, freezing in all of the structural information, the new bulk viscosity at t_1 can be calculated by bringing the temperature back to the original experimental temperature and letting the system relax to equilibrium. The initial conditions for the second time the system is relaxed will contain the modified chemical potentials [Eq. (39)] that correspond to a change in the driving force for relaxation. Once the system has relaxed, the bulk viscosity at t_1 can be calculated using Eq. (40). For a system that relaxes monotonically as a stretched exponential one can deduce that the viscosity measured at each point in time will monotonically increase as the system relaxes. Additionally, once the system has completely equilibrated, the bulk viscosity of the supercooled liquid can only be calculated by imposing an external hydrostatic stress since there are no internal driving forces generating stress.

The concept of structural units introducing internal stresses in a glass is not unfounded with regard to its microscopic origins. Atomic level stress has seen extensive work dating back nearly three decades, and an excellent survey of atomic level stress in the context of glass has been published by Egami [63] (and references therein). Atomic level stress is defined as a first order local response in energy to an affine strain and is merely a reflection of the disequilibrium of atoms with respect to their local environment. A recent molecular dynamics study on sodium silicates by Song *et al.* [64] presents an excellent case study because the authors reported a power law relationship between the magnitude of internal stress developed per atom and the cooling rate. The predominant stress was hydrostatic in nature which is in good agreement with what is being proposed in this work; the specific salient structural units were found to be topologically over constrained small (<6 membered) rings that experienced internal stress and were driven to grow in size in order to relax the stress. More broadly it was proposed that volumetric strain energy arises from radial misfit in nondirectionally bonded glasses (with high coordination numbers) and from angular misfits in glasses with highly directional bonds (with low coordination numbers). These points merely reinforce the authors' selection of the "structural and superstructural units" terminology as the underlying structural transformations are specific to the chemistry of the glass under consideration. It is merely a term used in lieu of a well-developed, widely accepted and chemistry-agnostic microscopic mechanism that quantifies such local excitations in energy.

V. THERMODYNAMIC BASIS FOR THE KINETIC INTERPRETATION OF FICTIVE TEMPERATURE

In this section the solutions to the rate equations will be discussed and a relationship between this solution and the Prony series will be established. The solution to the system of coupled first order differential equations [Eq. (36)] takes

the form

$$\alpha_i(t) = \sum_{m=1}^{n+1} c_m x_i^{(m)} e^{-\lambda_m t}, \quad (41)$$

where c_m 's are constants, $x_i^{(m)}$ is the i th element of the m th eigenvector ($\mathbf{x}^{(m)}$) of the phenomenological coefficient matrix \mathbf{M} , and λ_m is the m th eigenvalue of \mathbf{M} . After accounting for temporal boundary values [$\alpha_1(t=0) = v(t=0) - v^0$ and $\alpha_1(t \rightarrow \infty) = 0$] and introducing a characteristic relaxation rate $\lambda^* = 1/\tau_k$ in the exponent, one arrives at the following solution:

$$\phi(t) = \frac{v(t) - v^0}{v(t=0) - v^0} = \sum_{m=1}^{n+1} w_m e^{-(\lambda_m/\lambda^*)(t/\tau_k)}, \quad (42)$$

which is a weighted sum of exponentials with individual relaxation times $\tau_m = 1/\lambda_m$ and weights

$$w_m = \frac{c_m x_1^{(m)}}{\sum_{m=1}^{n+1} c_m x_1^{(m)}}. \quad (43)$$

For Eq. (42) to be expressed as a Prony series representation, we will have to impose the additional constraint that $c_m x_1^{(m)} > 0 \forall m$. If there are values of $c_m x_1^{(m)} < 0$, the summation in Eq. (41) for $i = 1$ will have to be partitioned into a difference of two sums and renormalized [using Eq. (43)] so as to obtain the difference of two weighted Prony series representations,

$$\begin{aligned} \phi(t) &= \frac{v(t) - v^0}{v(t=0) - v^0} \\ &= \frac{v(t=0)}{v(t=0) - v^0} \sum_{p=1}^{k_1} w_p^+ e^{-(\lambda_p^+/\lambda^*)(t/\tau_k^+)} \\ &\quad - \frac{v^0}{v(t=0) - v^0} \sum_{p=1}^{k_2} w_p^- e^{-(\lambda_p^-/\lambda^*)(t/\tau_k^-)}. \end{aligned} \quad (44)$$

This will account for multiple distinct relaxation modes, compressed exponential relaxation [65], and nonmonotonic relaxation behavior. Nonmonotonic and monotonic relaxation behavior are therefore solely governed by the properties of the phenomenological coefficient matrix and the initial conditions of the problem (which is governed by the thermal history). Some of the possible scenarios are illustrated in Fig. 1 assuming that each Prony series approximates a stretched exponential. The authors propose that Eqs. (7)–(44) present a formal thermodynamic theory for structural relaxation, and the solution to the set of coupled first order differential equations directly yield a Prony series, thus cementing the thermodynamic origin of the Prony series to model nonexponential structural relaxation. *However, we would like to re-emphasize here that the solutions presented in Eqs. (42)–(44) can result in a whole host of relaxation responses and aren't necessarily limited to a stretched exponential.*

One is therefore compelled to consider the implications of the specific case for which all of the w_m 's are positive [Eq. (42)]. The kinetic coefficient matrix is positive definite implying that all of the eigenvalues are real and positive; however, this does not imply that the first element in all of

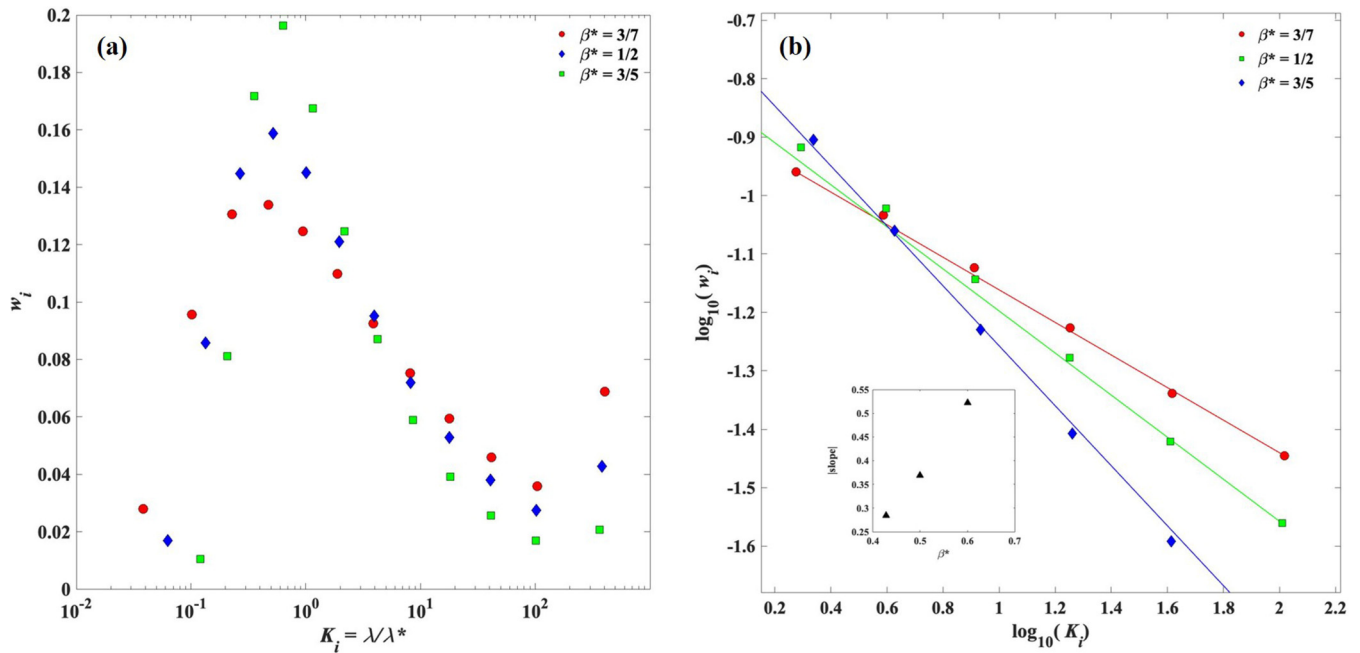


FIG. 2. (a) 12-term Prony series optimized to a stretched exponential by Mauro and Mauro [50] for different values of the stretching exponent. The optimized weights as a function of the exponents appear to follow an uncharacterized probability mass function with a unimodal peak on a semilogarithmic axis. (b) The tails of this mass function exhibit power law scaling over two decades of normalized frequencies and (inset) the magnitude of the slopes of lines on a double-logarithmic plot are linearly related to the stretching exponent.

the eigenvalue vectors are positive. Therefore, all of the w_m 's are positive only when $x_1^{(m)}$ and corresponding c_m do not have opposing signs. If \mathbf{c} denotes the vector of constants c_m , \mathbf{X} is the matrix containing column vectors of eigenvectors $\mathbf{x}^{(m)}$, and α_0 is the vector containing the initial values of α_i 's, then Eq. (41) would imply that $\mathbf{c} = \mathbf{X}^{-1}\alpha_0$. Therefore, the sign of the constants is sensitive to the initial conditions in addition to the eigenvectors of the phenomenological coefficient matrix \mathbf{M} . This imposes very specific constraints on the initial concentrations of structural and superstructural units as well as their kinetics in order to achieve nonexponential relaxation! In the high temperature regime, the stability of structural and superstructural units will be extremely low and therefore their interconversion nonexistent. This will result in a single ordinary differential equation governing the relaxation response. Therefore, the high temperature response will be a simple exponential, i.e., $\beta^*(T) \rightarrow 1$ and $\tau_k(T) = 1/M_{11}(T)$. Since the nature of the relaxation response in the intermediate temperature range is governed by the temperature dependence of the phenomenological coefficients and the initial concentrations of structural units which are system specific, the temperature dependence of β^* cannot be characterized with certainty in this temperature range assuming the response is going to be a stretched exponential.

Further insights may be drawn from the results of fitting a 12-term Prony series [50] that has been illustrated in Fig. 2. The parameters were optimized to fit the stretched exponential function and it was found that the weights w_i plotted as a function of the exponents K_i yielded a particular type of scaling law for different values of stretching exponents. On further inspection one observes that the tails [$w_i(K_i > 10^0)$] of the plot (apart from the farthest point on the right) scale as a power law with slopes proportional to the stretching

exponent itself. In fact, one of the main results from Ref. [50], illustrated in Fig. 2, shows that the Prony series converges to a stretched exponential only under specific values for the weights w_i and exponents K_i . It is also worth noting that the normalization constraint on w_i (i.e., $\sum_i w_i = 1$) implies that it may be interpreted as a probability mass function. Why must this be the case and is it of any physical significance? Is this scale-invariance symmetry in the optimized Prony series weights related to the aforementioned constraints imposed on the initial condition of structural and superstructural units and their kinetics? The following section will establish a link between the optimized parameters of the Prony series and the discrete and continuous analogs of a family of statistical distributions known as Lévy Stable distributions [66], which describe the underlying distribution of relaxation rates for a stretched exponential response. Relevant information regarding these distributions will be elucidated as the discussions unfold, however, it is recommended that the reader revert to the enclosed references for more information and insights.

Before moving on to this discussion, however, it is vital to establish a more physical understanding of the Prony series. A simple interpretation of the Prony series will be presented here in the context of a relaxation experiment. Consider a relaxation experiment being performed on a system possessing a characteristic relaxation time τ_k and corresponding characteristic relaxation rate $\lambda^* = 1/\tau_k$. This experiment is being conducted in the frequency domain wherein one is observing (making measurements of) the system at discrete, integral multiples ($n = 0, 1, \dots, m$) of some fixed observation frequency λ_{obs} , as one does in spectroscopy experiments [67–69]. Realistically, m and λ_{obs} must be finite and λ_{obs} has the additional constraint that it cannot be close to zero (static condition, corresponding to an infinite observation time for

any n). It is assumed that the system has a continuous distribution of relaxation rates $w(\lambda)$ supported on the positive half of the real line which is uniquely determined by the energy landscape of the system at a given temperature. To scale the sampling frequency for a relaxation experiment, the distribution of relaxation rates is normalized such that $w(\lambda) \rightarrow w(\lambda/\lambda^*)$. Therefore, for a given distribution of relaxation rates and experimental sampling frequencies, one obtains the sampled, discretized distribution of relaxation rates given by

$$w_d(\lambda/\lambda^*) = \sum_{n=0}^m w(\lambda/\lambda^*) \delta(\lambda/\lambda^* - n\lambda_{\text{obs}}/\lambda^*), \quad (45)$$

where $\delta(x)$ is defined as the Dirac delta function of an argument x . Taking the Laplace transform on both sides, one obtains the normalized time domain response of the relaxing system,

$$W_d(t/\tau_k) = \mathcal{L}\{w_d(\lambda/\lambda^*)\} = \sum_{n=0}^m w(n\lambda_{\text{obs}}/\lambda^*) e^{-(t/\tau_k)(n\lambda_{\text{obs}}/\lambda^*)}. \quad (46)$$

Substituting $z = e^{(t/\tau_k)(\lambda_{\text{obs}}/\lambda^*)}$ into Eq. (46), in the limit $m \rightarrow \infty$, one obtains the unilateral z transform of the distribution of relaxation rates [$w(\lambda/\lambda^*)$],

$$W_d(z) = \sum_{n=0}^{\infty} w(n\lambda_{\text{obs}}/\lambda^*) z^{-n}, \quad (47)$$

which is known to be the discrete analog of the Laplace transform. Again, Eq. (46) may be modified in the limit $m \rightarrow \infty$ with infinitely small increments in observation frequency [$\Delta(\lambda/\lambda^*) \rightarrow 0$] to obtain the Laplace transform of $w(\lambda/\lambda^*)$ that yields the time domain response of the relaxing system,

$$\begin{aligned} W(t/\tau_k) &= \lim_{\Delta(\lambda/\lambda^*) \rightarrow 0} W_d(t/\tau_k) \Delta(\lambda/\lambda^*) \\ &= \int_0^{\infty} w(\lambda/\lambda^*) e^{-(t/\tau_k)(\lambda/\lambda^*)} d(\lambda/\lambda^*). \end{aligned} \quad (48)$$

One may modify the index in Eq. (46) from n to $j = 1, 2, \dots, m$ such that $w_j(K_j)$ corresponds to some $K_j = n\lambda/\lambda^*$, $i = 1, 2, \dots, m$ to obtain a Prony series with m terms,

$$M(t) = \sum_{j=1}^m w_j(K_j) e^{-K_j(t/\tau_k)}. \quad (49)$$

Therefore, the Prony series is interpreted as a discrete version of a Laplace transform of a distribution of nondimensional (normalized) relaxation rates that is subject to experimental observation time constraints. For $0 \leq M(t) \leq 1$, we normalize the weights such that $\sum_j w_j(K_j) = 1$ is interpreted as a probability mass function of nondimensional relaxation rates, K_j . Referring to the equations presented in the thermodynamic model, these K_j 's are related to the eigenvalues of the phenomenological coefficient matrix and it is proposed that the weights w_j , composed of the eigenvectors and initial conditions, are functions of the eigenvalues. The eigenvalues of the kinetic coefficient represent the characteristic rate (and therefore timescale) of salient structural transformations during the relaxation process.

VI. DISTRIBUTION OF RELAXATION RATES, RELAXATION TIMES, AND ENERGY BARRIER HEIGHTS

Now consider a stretched exponential time domain response on the left hand side of Eq. (48). This corresponds to a case where there are a large number ($m \rightarrow \infty$) of structures and superstructures whose concentrations evolve in time and are kinetically coupled to the volume. Additionally, the increments in observation frequency are infinitesimally small, which is to say that we are interested in deriving the continuous distribution of relaxation rates (a probability density function) underlying the stretched exponential response. This will lead to the following Laplace transform of relaxation rates:

$$\begin{aligned} \phi(t) &= \exp \left[- \left(\frac{t}{\tau_k} \right)^{\beta^*} \right] \\ &= \int_0^{\infty} w(\lambda/\lambda^*) \exp \left(- \frac{\lambda}{\lambda^*} \frac{t}{\tau_k} \right) d(\lambda/\lambda^*). \end{aligned} \quad (50)$$

Then, $w(\lambda/\lambda^*)$ can be obtained through the Bromwich integral (inverse Laplace transform) of the stretched exponential function,

$$w(\lambda/\lambda^*) = \frac{1}{2\pi i} \int_{-i\infty}^{i\infty} e^{-(t/\tau_k)\beta^*} e^{(\lambda/\lambda^*)(t/\tau_k)} d(t/\tau_k). \quad (51)$$

Changing the variable to $u = -i(t/\tau_k)$ allows one to express $w(\lambda/\lambda^*)$ as a Fourier transform,

$$w(\lambda/\lambda^*) = l_{\beta^*}(\lambda/\lambda^*) = \frac{1}{2\pi} \int_{-\infty}^{\infty} e^{-(iu)\beta^*} e^{i(\lambda/\lambda^*)u} du. \quad (52)$$

The resulting integral in Eq. (52) does not have a simple analytical solution but has been shown to be in the domain of attraction of an *asymmetric* Lévy (α stable) distribution [70–74] for $\beta^* \in (0, 1]$ denoted $l_{\beta^*}(\lambda/\lambda^*)$. Lévy stable distributions do not possess simple analytical distributions but have a well-defined characteristic function. This family of distributions is commonly encountered in multiscale phenomena and enjoys the property of power-law tails (fractal like scaling [75,76]) with tails that decay as $l_{\beta^*}(x) \sim x^{-\beta^*-1}$. This has been illustrated in Fig. 5 in the Appendix. They also possess the property of stability under addition, which is to say that a random variable given by the sum of independent identically distributed random variables drawn from a stable distribution will be stably distributed [77] and is therefore a generalization of the central limit theorem. Detailed descriptions of stable distributions and their applications have been discussed in Refs. [77–80], and specific applications to the physics of relaxation may be found in Refs. [70,71,73,81]. For the discrete analog of these distributions, Refs. [82–84] served as primary references for this work and they are usually encountered in the context of scale-free networks [85].

Stable distributions are characterized by four parameters, viz., the first shape parameter $\beta^* \in (0, 2]$ (usually denoted α in the literature, hence the name α -stable distributions), second shape parameter $\beta \in [-1, 1]$, scale parameter $\gamma \in (0, \infty)$, and location parameter $\delta \in (-\infty, \infty)$. The second shape parameter determines the asymmetry of the distribution, i.e., the distribution is a symmetric stable distribution for

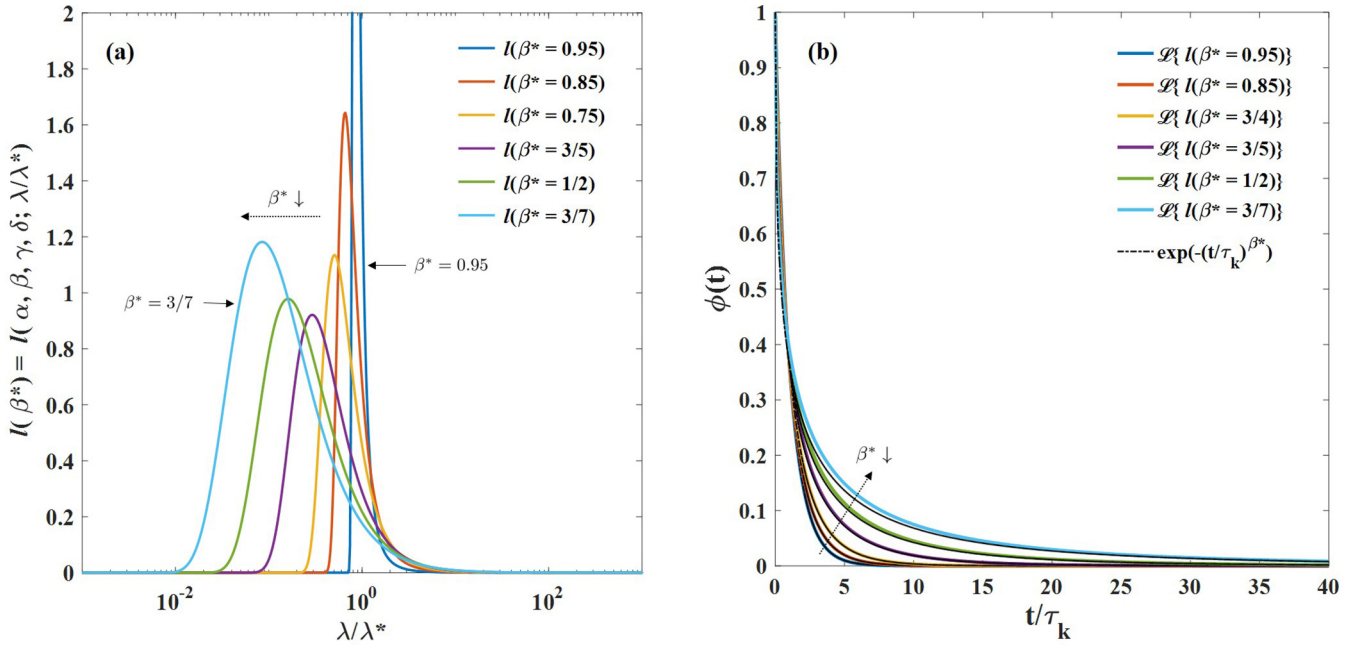


FIG. 3. (a) Asymmetric Lévy stable distributions for select shape parameters (stretching exponent) (β^*), and (b) The corresponding Laplace transforms the distributions (solid-colored lines). The stretched exponential function has also been plotted for all the shape parameters (dashed black lines) to show that the Laplace transforms of the distributions are almost identical to the function itself. The dotted arrows labeled “ $\beta^* \downarrow$ ” indicate the direction of decreasing β^* in both figures.

$\beta = 0$, completely asymmetric with a left tail for $\beta = -1$, and completely asymmetric with a right tail for $\beta = 1$. As mentioned above, the value of β^* is capped at 1 for the asymmetric case. Lévy stable distributions have a well-defined characteristic function but do not possess simple analytical expressions for probability densities with the exception of the Gaussian distribution for $\beta^* = 2(\beta = 0)$ and the Cauchy distribution for $\beta^* = 1(\beta = 0)$.

Subsequently, we will use the notation $l(\beta^*, \beta, \gamma, \delta)$ to refer to a general Lévy stable distribution with shape parameter β^* and $l_{\beta^*}(\lambda/\lambda^*)$ will be used as a shorthand to refer to the asymmetric Lévy distributions with right tails i.e., $l(\beta^*, \beta = 1, \gamma, \delta)$. Stable distribution parameters for a range $0.4 < \beta^* < 0.96$ were fit using Eqs. (50)–(52) using a nonlinear least squares fitting function in MATLAB. The details of the parametrization as well as specific libraries (including equivalent libraries in Python such as Ref. [86]) used have been provided in the Appendix. The optimized value of the shape parameter is referred to as α . Upon optimizing the parameters of the distribution, one finds that the condition $\alpha = \beta^*$ shows a slight deviation. This is discussed in more detail in the Appendix. These distributions and their Laplace transforms have been plotted in Fig. 3.

Owing to the relationship between the Lévy stable laws and the weights of the Prony series, one could expect to find qualitative similarities between the two. The qualitative similarities between the discrete and continuous cases are quite clear for $\beta^* = 3/7, 1/2$, and $3/5$. However, there are certain systematic differences that need to be pointed out. In the discrete case one observes that the normalized frequencies (K_i) appear to be the same at higher frequencies for different values of β^* , and one only begins to notice a systematic shift at lower K_i values as β^* decreases. This implies that the optimized

values for observation frequency are being weighted to longer observation times for processes that relax with lower β^* values. This shift towards lower values of normalized frequency is more apparent in the continuous case and is determined by the decrease in the location parameter δ of the Lévy stable distribution with a decrease in β^* . Another anomaly in the w_i values for the discrete case is the characteristic jump in the highest frequency value. This does not appear in the continuous case and this may be ascribed to the fact that the continuous distribution has a finite probability at very high frequencies owing to the fat tails of the distributions. This must be compensated for in the case of the optimized Prony series and is done by increasing the weight given to the fastest observation frequency.

The question of the distribution of relaxation times for stretched exponential relaxation is of importance to modeling relaxation as well as gathering structural insights on microscopic mechanisms that generate these distributions when applied to specific glass chemistries. When it is known that a random variable $\tilde{\lambda}$ (representing the nondimensional relaxation rates, λ/λ^*) is related to the random variable $\tilde{\tau}$ (representing the nondimensional relaxation times, τ/τ_k) as $\tilde{\tau} = \tilde{\lambda}^{-1}$, and that $\tilde{\lambda}$ is distributed as $\tilde{\lambda} \sim l_{\beta^*}(\lambda/\lambda^*)$, the distribution of relaxation times can then be derived,

$$\begin{aligned}
 P(\tau/\tau_k) &= \frac{1}{2\pi(\tau/\tau_k)^2} \int_{-\infty}^{\infty} e^{-(iu)^{\beta^*}} e^{i(\tau/\tau_k)^{-1}u} du \\
 &= (\tau/\tau_k)^{-2} l_{\beta^*}[(\tau/\tau_k)^{-1}].
 \end{aligned}
 \tag{53}$$

The details of the derivation for the distribution of relaxation rates and energy barrier heights have been included in the Appendix. The distribution of relaxation times has

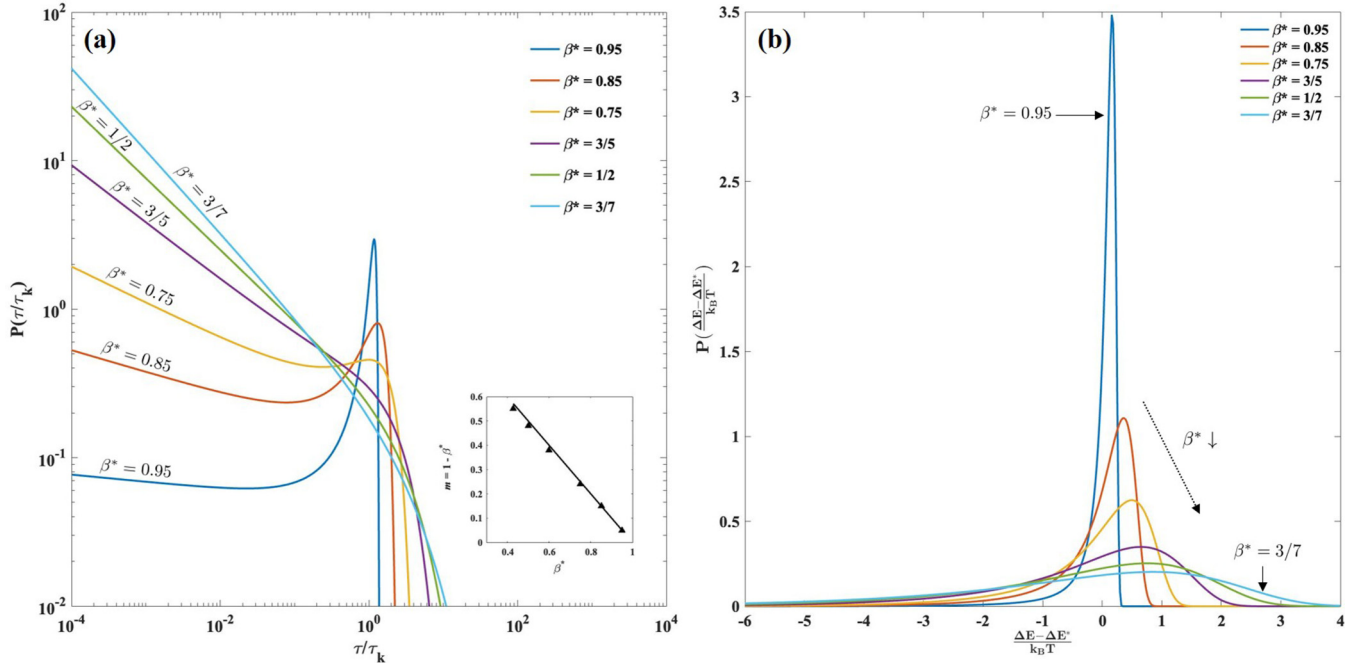


FIG. 4. (a) Distribution of relaxation times for select values of shape parameter (stretching exponent) β^* . It is seen that the left tails scale as power laws $P(\tilde{\tau}) \sim \tilde{\tau}^{-(1-\beta^*)}$. (b) The distribution of energy barrier heights for select values of shape parameter (stretching exponent) β^* . The dotted arrow labeled “ $\beta^* \downarrow$ ” indicates that β^* decreases (values indicated in the legend) as the peak of the distribution decreases and width of the distribution increases.

been illustrated in Fig. 4(a). It is seen that the mass of these distributions starts out centered around the characteristic relaxation time τ_k in the high temperature limit of $\beta^* \rightarrow 1$, implying a single relaxation time. The mass is then transferred over to the left tails of the distribution increasing nonexponentiality wherein the tails scale as a power law $P(\tilde{\tau}) \sim \tilde{\tau}^{-(1-\beta^*)}$, indicative of a transition to self-similar dynamics. This is equivalent to the distribution derived by Montroll and Bendler [Eq. (51d) in Ref. [81]] and the distribution derived by Richert and Richert [Eq. (8) in Ref. [87]] for the special case of $\beta_{\text{intr}} \rightarrow 1$.

The potential energy (or enthalpy) landscape description of glassy dynamics has been abundantly useful in modeling glassy systems and there is still much to gather from the topography of landscapes for glasses [2,52,88–90]. The kinetics of transitioning from one inherent structure to another is governed by the energy barrier height between two inherent structures, and the dynamics of the system in general will be governed by the distribution of energy barrier heights that the system samples at a given temperature and pressure. The distribution of inherent structure enthalpies has been shown to be Gaussian in glassy selenium for example [91], but the distribution of barrier heights has been assumed to be Gaussian [44] in theoretical models in the past, and in this light would be rather useful to quantify. A previous attempt at deriving a continuous distribution of energy barrier heights for stretched exponential relaxation was carried out by Liebovitch *et al.* [74] wherein an expression for the distribution of reaction rates was produced but was not explicitly extended to energy barrier distributions. Here an explicit expression for the distribution of energy barrier heights (that may be sampled for a given β^*) relative to a characteristic barrier ΔE^* is derived assuming the validity of

the Boltzmann factor for the transition rate from one arbitrary state on the landscape to another,

$$\lambda = \nu_0 \exp\left(-\frac{\Delta E}{k_B T}\right), \quad (54)$$

where ν_0 is an attempt frequency, k_B is the Boltzmann constant, and ΔE is the activation barrier (or potential energy, or enthalpy barrier) the system must overcome to transition from one state to another. Therefore, knowing the distribution of the random variable $\tilde{\lambda}$ and that the relationship between $\tilde{\lambda}$ and the random variable for the nondimensional energy barrier height \tilde{E} is $\tilde{E} = -\ln(\tilde{\lambda})$,

$$\tilde{E} = \frac{(\Delta E - \Delta E^*)}{k_B T}. \quad (55)$$

Here ΔE^* is the barrier height associated with the characteristic frequency λ^* in the context of Eq. (54). The following distribution for \tilde{E} is then derived:

$$\begin{aligned} P\left(\frac{\Delta E - \Delta E^*}{k_B T}\right) \\ = \exp\left(-\frac{\Delta E - \Delta E^*}{k_B T}\right) l^{\beta^*} \left[\exp\left(-\frac{\Delta E - \Delta E^*}{k_B T}\right) \right]. \end{aligned} \quad (56)$$

The distribution has been illustrated for different values of β^* in Fig. 4(b). Again, the mass of the distribution of barrier heights is heavily centered around $\tilde{E} = 0$ indicating that there is only a single barrier in the Debye relaxation limit. The distribution then broadens asymmetrically with increasing nonexponentiality.

VII. DISCUSSION

A general microscopic theory of relaxation has been a longstanding problem in condensed matter physics. The connection between structural relaxation and bulk viscous flow has been addressed in a macroscopic sense, and for the case of stretched exponential relaxation, the unequivocal presence of temporal self-similarity is highlighted. However, how does one use this information to synthesize a general microscopic theory for relaxation in glassy systems that is consistent across a wide range of temperatures over which nonexponential relaxation persists? Numerous computational and experimental investigations have been carried out to characterize the nature of cooperatively rearranging regions in glasses, a term popularized by the Adam-Gibbs (AG) [92] model for viscosity. Additionally, the nature and length scale of dynamic heterogeneities in supercooled liquids has received tremendous attention [93]. A particularly relevant result in the cited studies is the presence of self-similar (fractal) clusters spanning a range of glassy systems such as two-dimensional binary Lennard-Jones supercooled liquids near the glass transition [94], organic glass formers and hard sphere systems [95], self-organized two-dimensional lattice based models intended to study self-organized phases in covalent glasses [96], and in networks of distorted icosahedra of CuZr metallic glasses [97]. With the ubiquitous presence of spatial scale invariance symmetry in these glass forming systems above and below the glass transition temperature, one is compelled to hypothesize a link between spatial and temporal scale invariance in these systems.

The topological characterization of glasses [37] provides a level of abstraction that may uniquely poise one to study glasses as a class of networks with emergent spatial scale invariance properties dictated by their temperature (and pressure) dependence of topology. The recent advances in topological characterization of driving forces for relaxation [64,98], a statistical mechanics framework for characterizing the topological fluctuations spearheaded by Kirchner *et al.* [99], and statistical mechanical modeling of specific glass chemistries to characterize superstructural units [100] when coupled with classical diffusion limited based models for stretched exponential relaxation [16] may offer a link between the spatial and temporal scale-invariance symmetries discussed here. The thermodynamic framework presented here already alludes to reactions that may very well be diffusion limited, but in an abstract “diffusion of excitations” sense as originally purported by Phillips. The thermodynamic characterization and quantification of such excitations will be critical in this regard. One must also take into account the emergence of fast β -relaxation modes [39] below the glass transition temperature. The presence of scale-invariant distribution of relaxation times compels one to ponder the implications of this invariance to scale on stretched exponential β relaxation, especially since the same lower limit of $\beta^* = 3/7$ was reported for room temperature relaxation in Ref. [39]. Regarding the slower α -relaxation regime, the paper contains validation for using volume-relaxation data to estimate bulk viscosity, which is quite sparse for glasses. The authors hope that this work engenders further investigation of the temperature dependence of bulk viscosity for glass. Outside of

volume relaxation experiments, the requirement of specialized high-pressure equipment precludes the measurement of this transport coefficient for glasses and there appears to be scope for innovation in this regard.

VIII. CONCLUSIONS

In conclusion, the authors would like to leave the reader with the following take-aways from this work:

(i) The processes of shear and bulk flow are markedly different sources of entropy generation in isotropic media that will correspond to disparities in the kinetics of the two processes. Samples under a combination of shear and hydrostatic loads will exhibit contributions from both processes.

(ii) The kinetics of the two processes are expected to be different under conditions, where there is a disparity between the configurational degrees of freedom that contribute to shear and dilatational strains.

(iii) The underlying driving forces for structural relaxation stem from internal hydrostatic stresses that are generated by chemical potential differences between the equilibrium and nonequilibrium mass fractions of structures and superstructures that are kinetically coupled to the volume. These will drive the volume relaxation even in the absence of an applied mean normal stress.

(iv) A formal thermodynamic basis has been presented for the Prony series representation of the stretched exponential function in glasses with physical meaning ascribed to the weights (or modal amplitudes) of the series thus cementing the validity of the kinetic interpretation of fictive temperature.

(v) The underlying dynamics may be attributed to inherent symmetry of self-similarity observed in myriad experimental and simulation studies of dynamic heterogeneities in glass forming supercooled liquids.

ACKNOWLEDGMENTS

The authors would like to thank P. Gupta for fruitful discussions at the outset of this work and E. D. Zanotto for helpful comments during the various stages of drafting this manuscript. The authors would also like to extend their gratitude to D. C. Allan, O. Gulbiten, and C. Wilkinson for insightful discussion at various stages of this work. The authors are also grateful for Corning Incorporated, the Department of Materials Science and Engineering and the Materials Research Institute at Penn State, for supporting this work.

APPENDIX

1. Lévy stable distributions and their parametrization

The asymmetric Lévy stable distribution naturally arises when we consider the case when a stretched exponential regression to equilibrium arises from multiple exponential relaxations with a distribution of relaxation rates,

$$\exp\left[-\left(\frac{t}{\tau_k}\right)^{\beta^*}\right] = \int_0^\infty l_{\beta^*}(\lambda/\lambda^*) \exp\left(-\frac{\lambda}{\lambda^*} \frac{t}{\tau_k}\right) d(\lambda/\lambda^*), \quad (\text{A1})$$

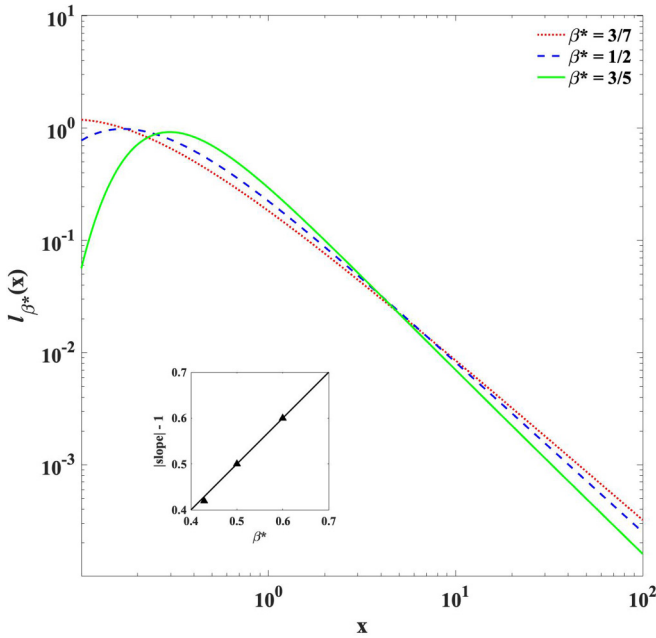


FIG. 5. Power law tails of the Lévy distribution (right tails of asymmetric distributions have been illustrated here) scale as $I_{\beta^*}(x) \sim x^{-(1+\beta^*)}$ as shown in the inset figure.

where β^* is the stretching exponent, τ_k is the characteristic relaxation time, λ is the relaxation rate, and λ^* is the characteristic relaxation rate. The resulting distribution of nondimensional relaxation rates is given by the integral

$$I_{\beta^*}(\lambda/\lambda^*) = \frac{1}{2\pi} \int_{-\infty}^{\infty} e^{-(iu)^{\beta^*}} e^{i(\lambda/\lambda^*)u} du. \quad (\text{A2})$$

The integral in Eq. (A2) does not have a simple analytical solution but has been shown to be in the domain of attraction of an *asymmetric* Lévy (α stable) distribution [70–74] for $\beta^* \in (0, 1]$ denoted $I_{\beta^*}(\lambda/\lambda^*)$. Lévy stable distributions do not possess simple analytical distributions but have a well-defined characteristic function. Lévy stable distributions must not be confused with the Lévy distribution which is a special case of the stable distribution. This family of distributions is commonly encountered in multiscale phenomena, and enjoys the property of power-law tails (fractal like scaling [75,76]) as illustrated in Fig. 5. These distributions also possess the property of stability under addition, which is to say that a random variable given by the sum of independent identically distributed random variables drawn from a stable distribution will be stably distributed [77] and this constitutes the generalization of the central limit theorem. Detailed descriptions of stable distributions and their applications have been discussed in Refs. [77–80], and specific applications to the physics of relaxation may be found in Refs. [70,71,73,81]. For the discrete analog of these distributions, Refs. [82–84] served as primary references for this work and they are usually encountered in the context of scale-free networks [85].

Stable distributions are characterized by four parameters, viz., the first shape parameter $\beta^* \in (0, 2]$ (usually denoted α in the literature, hence the name α -stable distributions), second shape parameter $\beta \in [-1, 1]$, scale parameter $\gamma \in (0, \infty)$, and location parameter $\delta \in (-\infty, \infty)$. The second

shape parameter determines the asymmetry of the distribution, i.e., the distribution is a symmetric stable distribution for $\beta = 0$, completely asymmetric with a left tail for $\beta = -1$, and completely asymmetric with a right tail for $\beta = 1$. As mentioned above, the value of β^* is capped at 1 for the asymmetric case. Lévy stable distributions have a well-defined characteristic function but do not possess simple analytical expressions for probability densities with the exception of the Gaussian distribution for $\beta^* = 2$ ($\beta = 0$) and the Cauchy distribution for $\beta^* = 1$ ($\beta = 0$).

In practice, we have found that the numerical evaluation of such integrals or equivalent summations were computationally intensive and unstable at higher values. However, MATLAB possesses a stable distribution function that evaluates the value of the distribution function given the values of the parameters. The integral in Eq. (A2) was evaluated over a limited range and the data were used to fit the stable distribution parameters for a range $0.4 < \beta^* < 0.96$ in MATLAB using a nonlinear least squares function. Additionally, polynomial fits for each of the parameters as a function of β^* were identified so that the parameter values may be interpolated for nonparametrized values of β^* in the interval $[0.4, 0.96]$. In practice, the shape parameter that is obtained when fit to data from Eq. (A2) (which we will denote as α) deviates slightly from β^* used in Eq. (A2). In theory, they are expected to be equal, but we attribute this small difference to minor numerical errors. The polynomial equations obtained from regression for the stable distribution parameters are

$$\begin{aligned} \alpha &= 0.1555\beta^{*3} - 0.2988^2 + 1.1447\beta^*, \\ \beta &= 1, \\ \gamma &= -3.3282\beta^{*2} + 5.3476\beta^* - 0.38, \\ \delta &= 3.5278\beta^{*4} - 7.9012\beta^* + 4.5135\beta^{*2} \\ &\quad + 0.0003\beta^* + 0.0037. \end{aligned} \quad (\text{A3})$$

Finally we note that there is an equivalent Python package that has been developed to handle calculations related to stable distributions [86], but we had to forego using this because of documented issues with fitting distributions below shape parameters of 0.5.

2. Distribution of relaxation times and energy barrier heights

The probability that the random variable $\tilde{\tau}$, a nondimensional relaxation time, lies between in the interval $[(\tau/\tau_k), (\tau/\tau_k) + d(\tau/\tau_k)]$ is

$$\text{Pr}[(\tau/\tau_k) < \tilde{\tau} < (\tau/\tau_k) + d(\tau/\tau_k)] = P(\tau/\tau_k)d(\tau/\tau_k), \quad (\text{A4})$$

where $P(\tau/\tau_k)$ is the probability density function (PDF) of relaxation times. In this section, we are tasked with deriving $P(\tau/\tau_k)$ given that $\tilde{\tau} = \tilde{\lambda}^{-1}$, where $\tilde{\lambda}$ is a random variable that represents the nondimensional relaxation rate and is known to be distributed as an asymmetric Lévy stable distribution defined as

$$I_{\beta^*}(\lambda/\lambda^*) = \frac{1}{2\pi} \int_{-\infty}^{\infty} e^{-(iu)^{\beta^*}} e^{i(\lambda/\lambda^*)u} du, \quad (\text{A5})$$

where

$$\text{Pr}[(\lambda/\lambda^*) < \tilde{\lambda} < (\lambda/\lambda^*) + d(\lambda/\lambda^*)] = l_{\beta^*}(\lambda/\lambda^*)d(\lambda/\lambda^*).$$

The corresponding cumulative distribution (CDF) function is given by integrating Eq. (A5),

$$F_{\beta^*}(\tilde{\lambda} \leq \lambda/\lambda^*) = \frac{1}{2\pi} \int_0^{\lambda/\lambda^*} \int_{-\infty}^{\infty} e^{-(iu)^{\beta^*}} e^{i(\lambda/\lambda^*)u} dud(\lambda/\lambda^*),$$

$$F_{\beta^*}(\tilde{\lambda} \leq \lambda/\lambda^*) = \frac{1}{2\pi} \int_{-\infty}^{\infty} (iu)^{-1} e^{-(iu)^{\beta^*}} (e^{i(\lambda/\lambda^*)u} - 1) du. \quad (\text{A6})$$

We now turn our attention to the CDF of $\tilde{\tau}$ given by $F(\tilde{\tau} \leq \tau/\tau_k)$. Knowing the relationship between $\tilde{\tau}$ and $\tilde{\lambda}$ we can infer that

$$F(\tilde{\tau} \leq \tau/\tau_k) = F[\tilde{\lambda} \geq (\tau/\tau_k)^{-1}],$$

$$F(\tilde{\tau} \leq \tau/\tau_k) = 1 - F_{\beta^*}[\tilde{\lambda} \leq (\tau/\tau_k)^{-1}]. \quad (\text{A7})$$

Therefore, $P(\tau/\tau_k)$ is the derivative of Eq. (A7) with respect to (τ/τ_k) ,

$$P(\tau/\tau_k) = -\frac{d}{d(\tau/\tau_k)} F_{\beta^*}[\tilde{\lambda} \leq (\tau/\tau_k)^{-1}]$$

$$= -\frac{1}{2\pi} \frac{d}{d(\tau/\tau_k)} \left\{ \int_{-\infty}^{\infty} (iu)^{-1} e^{-(iu)^{\beta^*}} (e^{i(\tau/\tau_k)^{-1}u} - 1) du \right\}, \quad (\text{A8})$$

yielding the following PDF for the distribution of relaxation times:

$$P(\tau/\tau_k) = \frac{1}{2\pi(\tau/\tau_k)^2} \int_{-\infty}^{\infty} e^{-(iu)^{\beta^*}} e^{i(\tau/\tau_k)^{-1}u} du$$

$$= (\tau/\tau_k)^{-2} l_{\beta^*}[(\tau/\tau_k)^{-1}]. \quad (\text{A9})$$

Similarly, we may derive the PDF of sampled energy barrier heights on an energy landscape by assuming that the transition rate (or relaxation rate) λ associated with an energy

barrier ΔE of transitioning from one state to another in phase space is given by

$$\lambda = \nu_0 \exp\left(-\frac{\Delta E}{k_B T}\right), \quad (\text{A10})$$

where ν_0 is an attempt frequency, k_B is the Boltzmann constant, and T is the absolute temperature. Here it is assumed that the system is sampling a particular distribution of energy barrier heights at a given temperature and the resulting structural changes are distributed over a range of relaxation times. Now accounting for the characteristic relaxation rate, we may derive an expression for the nondimensional relaxation rate,

$$\frac{\lambda}{\lambda^*} = \exp\left(-\frac{(\Delta E - \Delta E^*)}{k_B T}\right). \quad (\text{A11})$$

We now treat the absolute value of the term within the exponential as a random variable \tilde{E} and from Eq. (A11), its relationship with $\tilde{\lambda}$ is

$$\tilde{E} = -\ln(\tilde{\lambda}). \quad (\text{A12})$$

In a similar fashion as in Eq. (A7), we infer that

$$F\left(\tilde{E} \leq \frac{(\Delta E - \Delta E^*)}{k_B T}\right)$$

$$= F\left[\tilde{\lambda} \geq \exp\left(-\frac{(\Delta E - \Delta E^*)}{k_B T}\right)\right],$$

$$F\left(\tilde{E} \leq \frac{(\Delta E - \Delta E^*)}{k_B T}\right)$$

$$= 1 - F_{\beta^*}\left[\tilde{\lambda} \leq \exp\left(-\frac{(\Delta E - \Delta E^*)}{k_B T}\right)\right]. \quad (\text{A13})$$

Following a similar procedure as in Eq. (A8) we arrive at the following PDF for the distribution of sampled energy barrier heights:

$$P\left(\frac{\Delta E - \Delta E^*}{k_B T}\right) = \exp\left(-\frac{\Delta E - \Delta E^*}{k_B T}\right) l_{\beta^*}$$

$$\times \left[\exp\left(-\frac{\Delta E - \Delta E^*}{k_B T}\right) \right]. \quad (\text{A14})$$

It is worth noting that this distribution is approximately a power law distribution truncated by an exponential decay.

- [1] P. W. Anderson, Through the glass lightly, *Science* **267**, 1615 (1995).
- [2] P. G. Debenedetti and F. H. Stillinger, Supercooled liquids and the glass transition, *Nature (London)* **410**, 259 (2001).
- [3] M. D. Ediger, C. A. Angell, and S. R. Nagel, Supercooled liquids and glasses, *J. Phys. Chem.* **100**, 13200 (1996).
- [4] C. A. Angell, K. L. Ngai, G. B. McKenna, P. F. McMillan, and S. W. Martin, Relaxation in glassforming liquids and amorphous solids, *J. Appl. Phys.* **88**, 3113 (2000).
- [5] E. D. Zanotto and J. C. Mauro, The glassy state of matter: its definition and ultimate fate, *J. Non-Cryst. Solids* **471**, 490 (2017).

- [6] L. Ding, M. Thieme, S. Demouchy, C. Kunisch, and B. J. P. Kaus, Effect of pressure and temperature on viscosity of a borosilicate glass, *J. Am. Ceram. Soc.* **101**, 3936 (2018).
- [7] L. Ding, S. Buhre, C. Kunisch, and B. Kaus, Pressure dependence of density and structural relaxation of glass near the glass transition region, *J. Am. Ceram. Soc.* **101**, 1149 (2018).
- [8] L. Ding, K. Doss, Y. Yang, K. H. Lee, M. Bockowski, S. Demouchy, M. Thieme, B. Ziebarth, Q. Wang, M. M. Smedskjaer, and J. C. Mauro, Volume relaxation in a borosilicate glass hot compressed by three different methods, *J. Am. Ceram. Soc.* **104**, 816 (2021).
- [9] J. C. Mauro, Grand challenges in glass science, *Front. Mater.* **1**, 20 (2014).

- [10] J. C. Mauro, C. S. Philip, D. J. Vaughn, and M. S. Pambianchi, Glass science in the united states: Current status and future directions, *Int. J. Appl. Glass. Sci.* **5**, 2 (2014).
- [11] A. Y. Sane and A. R. Cooper, Stress buildup and relaxation during ion exchange strengthening of glass, *J. Am. Ceram. Soc.* **70**, 86 (1987).
- [12] A. K. Varshneya and J. C. Mauro, *Fundamentals of Inorganic Glasses*, 3rd ed. (Elsevier, Amsterdam, Netherlands, 2019).
- [13] R. Kohlrausch, Theorie des elektrischen rückstandes in der leidener flasche, *Pogg. Ann. Phys. Chem.* **91**, 179 (1854).
- [14] M. Cardona, R. V Chamberlin, and W. Marx, The history of the stretched exponential function, *Ann. Phys. (Leipzig)* **16**, 842 (2007).
- [15] B. J. Cherayil, Stretched exponential relaxation in polymer dynamics, *J. Chem. Phys.* **97**, 2090 (1992).
- [16] J. C. Phillips, Stretched exponential relaxation in molecular and electronic glasses, *Rep. Prog. Phys.* **59**, 1133 (1996).
- [17] G. W. Scherer, *Relaxation in Glass and Composites* (Wiley, New York 1986).
- [18] K. Doss, C. J. Wilkinson, Y. Yang, K. H. Lee, L. Huang, and J. C. Mauro, Maxwell relaxation time for nonexponential α -relaxation phenomena in glassy systems, *J. Am. Ceram. Soc.* **103**, 3590 (2020).
- [19] R. Felipe Lancelotti, D. Roberto Cassar, M. Nalin, O. Peitl, and E. Dutra Zanotto, Is the structural relaxation of glasses controlled by equilibrium shear viscosity?, *J. Am. Ceram. Soc.* **104**, 2066 (2021).
- [20] S. M. Rekhson, Structural relaxation and shear stresses in the glass-transition region, *Sov. J. Glas. Phys. Chem.* **1**, 443 (1976).
- [21] M. J. Holmes, N. G. Parker, and M. J. W. Povey, Temperature dependence of bulk viscosity in water using acoustic spectroscopy, *J. Phys.: Conf. Ser.*, **269**, 012011 (2011).
- [22] A. S. Dukhin and P. J. Goetz, Bulk viscosity and compressibility measurement using acoustic spectroscopy, *J. Chem. Phys.* **130**, 124519 (2009).
- [23] K. F. Herzfeld, Bulk viscosity and shear viscosity in fluids according to the theory of irreversible processes, *J. Chem. Phys.* **28**, 595 (1958).
- [24] R. E. Graves and B. M. Argrow, Bulk viscosity: Past to present, *J. Thermophys. Heat. Trans.* **13**, 337 (1999).
- [25] F. Jaeger, O. K. Matar, and E. A. Müller, Bulk viscosity of molecular fluids, *J. Chem. Phys.* **148**, 174504 (2018).
- [26] J. P. Boon and S. Yip, *Molecular Hydrodynamics* (Dover, New York, 2013).
- [27] R. Zwanzig and R. D. Mountain, High-Frequency elastic moduli of simple fluids, *J. Chem. Phys.* **43**, 4464 (1965).
- [28] K. Trachenko and V. V. Brazhkin, Collective modes and thermodynamics of the liquid state, *Rep. Prog. Phys.* **79**, 016502 (2016).
- [29] K. Trachenko, Slow dynamics and stress relaxation in a liquid as an elastic medium, *Phys. Rev. B* **75**, 212201 (2007).
- [30] K. Trachenko and V. V. Brazhkin, Understanding the problem of glass transition on the basis of elastic waves in a liquid, *J. Phys.: Condens. Matter* **21**, 425104 (2009).
- [31] M. Potuzak, R. C. Welch, and J. C. Mauro, Topological origin of stretched exponential relaxation in glass, *J. Chem. Phys.* **135**, 214502 (2011).
- [32] X. Guo, J. C. Mauro, D. C. Allan, and M. M. Smedskjaer, Predictive model for the composition dependence of glassy dynamics, *J. Am. Ceram. Soc.* **101**, 1169 (2018).
- [33] Y. Yang, C. J. Wilkinson, K. H. Lee, K. Doss, T. D. Bennett, Y. K. Shin, A. C. T. Van Duin, and J. C. Mauro, Prediction of the glass transition temperatures of zeolitic imidazolate glasses through topological constraint theory, *J. Phys. Chem. Lett.* **9**, 6985 (2018).
- [34] M. M. Smedskjaer, J. C. Mauro, R. E. Youngman, C. L. Hogue, M. Potuzak, and Y. Yue, Topological principles of borosilicate glass chemistry, *J. Phys. Chem. B* **115**, 12930 (2011).
- [35] J. C. Mauro, A. J. Ellison, D. C. Allan, and M. M. Smedskjaer, Topological model for the viscosity of multicomponent glass-forming liquids, *Int. J. Appl. Glass. Sci.* **4**, 408 (2013).
- [36] J. C. Phillips and M. F. Thorpe, Constraint theory, vector percolation and glass formation, *Solid State Commun.* **53**, 699 (1985).
- [37] J. C. Mauro, Topological constraint theory, *Am. Ceram. Soc. Bull.* **90**, 31 (2011).
- [38] P. Grassberger and I. Procaccia, The long time properties of diffusion in a medium with static traps, *J. Chem. Phys.* **77**, 6281 (1982).
- [39] R. C. Welch, J. R. Smith, M. Potuzak, X. Guo, B. F. Bowden, T. J. Kiczanski, D. C. Allan, E. A. King, A. J. Ellison, and J. C. Mauro, Dynamics of Glass Relaxation at Room Temperature, *Phys. Rev. Lett.* **110**, 265901 (2013).
- [40] T. Förster, Experimentelle und theoretische untersuchung des zwischenmolekularen übergangs von elektronenanregungsenergie, *Z. Naturforsch. A* **4**, 321 (1949).
- [41] R. G. Palmer, D. L. Stein, E. Abrahams, and P. W. Anderson, Models of Hierarchically Constrained Dynamics for Glassy Relaxation, *Phys. Rev. Lett.* **53**, 958 (1984).
- [42] S. H. Glarum, Dielectric relaxation of polar liquids, *J. Chem. Phys.* **33**, 1371 (1960).
- [43] J. Klafter and M. F. Shlesinger, On the relationship among three theories of relaxation in disordered systems, *Proc. Natl. Acad. Sci. USA* **83**, 848 (1986).
- [44] V. Lubchenko and P. G. Wolynes, Theory of structural glasses and supercooled liquids, *Annu. Rev. Phys. Chem.* **58**, 235 (2007).
- [45] X. Xia and P. G. Wolynes, Microscopic Theory of Heterogeneity and Nonexponential Relaxations in Supercooled Liquids, *Phys. Rev. Lett.* **86**, 5526 (2001).
- [46] T. R. Kirkpatrick, D. Thirumalai, and P. G. Wolynes, Scaling concepts for the dynamics of viscous liquids near an ideal glassy state, *Phys. Rev. A* **40**, 1045 (1989).
- [47] J. D. Stevenson, J. Schmalian, and P. G. Wolynes, The shapes of cooperatively rearranging regions in glass-forming liquids, *Nat. Phys.* **2**, 268 (2006).
- [48] T. R. Kirkpatrick and D. Thirumalai, Colloquium: Random first order transition theory concepts in biology and physics, *Rev. Mod. Phys.* **87**, 183 (2015).
- [49] Z. Zheng, J. C. Mauro, and D. C. Allan, Modeling of delayed elasticity in glass, *J. Non-Cryst. Solids* **500**, 432 (2018).
- [50] J. C. Mauro and Y. Z. Mauro, On the prony series representation of stretched exponential relaxation, *Phys. A (Amsterdam, Neth.)* **506**, 75 (2018).

- [51] C. J. Wilkinson, Y. Z. Mauro, and J. C. Mauro, RelaxPy: Python code for modeling of glass relaxation behavior, *SoftwareX* **7**, 255 (2018).
- [52] J. C. Mauro, R. J. Loucks, and P. K. Gupta, Fictive temperature and the glassy state, *J. Am. Ceram. Soc.* **92**, 75 (2009).
- [53] X. Guo, M. Potuzak, J. C. Mauro, D. C. Allan, T. J. Kiczanski, and Y. Yue, Unified approach for determining the enthalpic fictive temperature of glasses with arbitrary thermal history, *J. Non-Cryst. Solids* **357**, 3230 (2011).
- [54] Y. Yue, R. Von der Ohe, and S. L. Jensen, Fictive temperature, cooling rate, and viscosity of glasses, *J. Chem. Phys.* **120**, 8053 (2004).
- [55] J. C. Mauro, D. C. Allan, and M. Potuzak, Nonequilibrium viscosity of glass, *Phys. Rev. B* **80**, 094204 (2009).
- [56] H. N. Ritland, Limitations of the fictive temperature concept, *J. Am. Ceram. Soc.* **12**, 403 (1956).
- [57] M. B. Nugroho, Initial results in prony analysis of power system response signals, *IEEE Trans. Power Syst.* **5**, 80 (1990).
- [58] P. K. Gupta and C. T. Moynihan, Prigogine – defay ratio for systems with more than one order parameter, *J. Chem. Phys.* **65**, 4136 (1976).
- [59] P. K. Gupta, Fictive pressure effects in structural relaxation, *J. Non-Cryst. Solids* **102**, 231 (1988).
- [60] X. Guo, M. M. Smedskjaer, and J. C. Mauro, Linking equilibrium and nonequilibrium dynamics in glass-forming systems, *J. Phys. Chem. B* **120**, 3226 (2016).
- [61] S. R. de Groot and P. Mazur, *Non-Equilibrium Thermodynamics* (North-Holland, Amsterdam, 1984).
- [62] K. Januchta and M. M. Smedskjaer, Indentation deformation in oxide glasses: Quantification, structural changes, and relation to cracking, *J. Non. Cryst. Solids X* **1**, 100007 (2019).
- [63] T. Egami, Atomic level stresses, *Prog. Mater. Sci.* **56**, 637 (2011).
- [64] W. Song, X. Li, B. Wang, N. M. Anoop Krishnan, S. Goyal, M. M. Smedskjaer, J. C. Mauro, C. G. Hoover, and M. Bauchy, Atomic picture of structural relaxation in silicate glasses, *Appl. Phys. Lett.* **114**, 233703 (2019).
- [65] A. Lattanzi, G. Dattoli, and G. Baldacchini, Physics and mathematics of the photoluminescence of complex systems, [arXiv:2012.04645v2](https://arxiv.org/abs/2012.04645v2).
- [66] P. Lévy, *Theorie de l'addition Des Variables Aléatoires* (Gauthier-Villars, Paris, 1937).
- [67] N. O. Birge and S. R. Nagel, Specific-Heat Spectroscopy of the Glass Transition, *Phys. Rev. Lett.* **54**, 2674 (1985).
- [68] B. Roling, Determination of divalent cation mobilities in glass by dynamic mechanical thermal analysis (dmta): Evidence for cation coupling effects, *Solid. State. Ion.* **105**, 47 (1998).
- [69] R. Böhmer, K. L. Ngai, C. A. Angell, and D. J. Plazek, Non-exponential relaxations in strong and fragile glass formers, *J. Chem. Phys.* **99**, 4201 (1993).
- [70] A. Jurlewicz and K. Weron, A relationship between asymmetric lévy-stable distributions and the dielectric susceptibility, *J. Stat. Phys.* **73**, 69 (1993).
- [71] K. Weron and A. Jurlewicz, Two forms of self-similarity as a fundamental feature of the power-law dielectric response, *J. Phys. A* **26**, 395 (1993).
- [72] K. Weron, A probabilistic mechanism hidden behind the universal power law for dielectric relaxation: General relaxation equation, *J. Phys.: Condens. Matter* **3**, 9151 (1991).
- [73] I. Koponen, Random transition rate model of stretched exponential relaxation, *J. Non-Cryst. Solids* **189**, 154 (1995).
- [74] L. S. Liebovitch and T. I. Tóth, Distributions of activation energy barriers that produce stretched exponential probability distributions for the time spent in each state of the two state reaction $A \rightleftharpoons B$, *Bull. Math. Biol.* **53**, 443 (1991).
- [75] B. B. Mandelbrot, *The Fractal Geometry of Nature* (W. H. Freeman, San Francisco, 1982).
- [76] K. Doss, A. S. Hanshew, and J. C. Mauro, Signatures of criticality in mining accidents and recurrent neural network forecasting model, *Phys. A (Amsterdam, Neth.)* **537**, 122656 (2020).
- [77] B. V. Gnedenko and A. N. Kolmogorov, *Limit Distributions for Sums of Independent Random Variables* (Addison-Wesley, Cambridge, MA, 1954).
- [78] W. Feller, *An Introduction to Probability Theory and Its Applications* (Wiley, New York, 1966).
- [79] J.-P. Bouchaud and M. Potters, *Theory of Financial Risk and Derivative Pricing*, 2nd ed. (Cambridge University Press, Cambridge, UK, 2003).
- [80] M. F. Shlesinger, G. M. Zaslavsky, and J. Klafter, Strange kinetics, *Nature (London)* **363**, 31 (1993).
- [81] E. W. Montroll and J. T. Bendler, On lévy (or stable) distributions and the williams-watts model of dielectric relaxation, *J. Stat. Phys.* **34**, 129 (1984).
- [82] W. H. Lee, K. I. Hopcraft, and E. Jakeman, Continuous and discrete stable processes, *Phys. Rev. E* **77**, 011109(4) (2008).
- [83] F. W. Steutel and K. van Harn, Discrete analogues of self-decomposability and stability, *Ann. Probab.* **7**, 893 (1979).
- [84] K. I. Hopcraft, E. Jakeman, and J. O. Matthews, Discrete scale-free distributions and associated limit theorems, *J. Phys. A* **37**, 635 (2004).
- [85] A. L. Barbási and R. Albert, Emergence of scaling in random networks, *Science* **286**, 509 (1999).
- [86] J. M. Miotto, Github: <https://github.com/josemiotto/pylevy>.
- [87] R. Richert and M. Richert, Dynamic heterogeneity, spatially distributed stretched-exponential patterns, and transient dispersions in solvation dynamics, *Phys. Rev. E* **58**, 779 (1998).
- [88] J. C. Mauro, S. S. Uzun, W. Bras, and S. Sen, Nonmonotonic Evolution of Density Fluctuations during Glass Relaxation, *Phys. Rev. Lett.* **102**, 155506 (2009).
- [89] J. C. Mauro, Effect of fragility on relaxation of density fluctuations in glass, *J. Non-Cryst. Solids* **357**, 3520 (2011).
- [90] M. D. Ediger and P. Harrowell, Perspective: Supercooled liquids and glasses, *J. Chem. Phys.* **137**, 080901 (2012).
- [91] J. C. Mauro and R. J. Loucks, Selenium glass transition: a model based on the enthalpy landscape approach and nonequilibrium statistical mechanics, *Phys. Rev. B* **76**, 174202 (2007).
- [92] G. Adam and J. H. Gibbs, On the temperature dependence of cooperative relaxation properties in glass-forming liquids, *J. Chem. Phys.* **43**, 139 (1965).
- [93] M. D. Ediger, Spatially heterogeneous dynamics in supercooled liquids, *Annu. Rev. Phys. Chem.* **51**, 99 (2000).
- [94] G. Johnson, A. I. Mel'cuk, H. Gould, W. Klein, and R. D. Mountain, Molecular-Dynamics study of long-lived structures in a fragile glass-forming liquid, *Phys. Rev. E* **57**, 5707 (1998).
- [95] S. A. Reinsberg, A. Heuer, B. Doliwa, H. Zimmermann, and H. W. Spiess, Comparative study of the nmr length scale

- of dynamic heterogeneities of three different glass formers, *J. Non-Cryst. Solids* **307–310**, 208 (2002).
- [96] M. A. Brière, M. V. Chubynsky, and N. Mousseau, Self-Organized criticality in the intermediate phase of rigidity percolation, *Phys. Rev. E* **75**, 056108 (2007).
- [97] Z. W. Wu, F. X. Li, C. W. Huo, M. Z. Li, W. H. Wang, and K. X. Liu, Critical scaling of icosahedral medium-range order in CuZr metallic glass-forming liquids, *Sci. Rep.* **6**, 35967 (2016).
- [98] X. Li, W. Song, M. M. Smedskjaer, J. C. Mauro, and M. Bauchy, Quantifying the internal stress in over-constrained glasses by molecular dynamics simulations, *J. Non-Cryst. Solids* **X 1**, 100013 (2019).
- [99] K. A. Kirchner, S. H. Kim, and J. C. Mauro, Statistical mechanics of topological fluctuations in glass-forming liquids, *Phys. A (Amsterdam, Neth.)* **510**, 787 (2018).
- [100] M. S. Bødker, J. C. Mauro, R. E. Youngman, and M. M. Smedskjaer, Statistical mechanical modeling of borate glass structure and topology: prediction of superstructural units and glass transition temperature, *J. Phys. Chem. B* **123**, 1206 (2019).